ELSEVIER

Journal of Luminescence 75 (1997) 183–192

JOURNAL OF LUMINESCENCE

Electron traps and transfer efficiency of cerium-doped aluminate scintillators

R.H. Bartram[a,*], D.S. Hamilton[a], L.A. Kappers[a], A. Lempicki[b,c]

[a] *Department of Physics and Institute of Materials Science, University of Connecticut, 2152 Hillside Rd., Storrs, CT 06269-3046, USA*

[b] *Department of Chemistry, Boston University, Boston, MA 02215, USA*

[c] *ALEM Associates, Boston, MA 02115, USA*

Received 10 March 1997; received in revised form 19 June 1997; accepted 19 June 1997

Abstract

Comparative measurements of thermoluminescence and scintillation light outputs of gamma-ray irradiated Ce:$LuAlO_3$ (LuAP) and Cc:$YAlO_3$ (YAP) revcal that electron trapping significantly depresses transfer efficiency in these scintillator materials, but fails to explain fully either their performance differential or their departures from ideal efficiency. In the limit of short radiation times, the ratio of integrated thermoluminescence light output to integrated scintillation light output is 0.14 in LuAP and 0.02 in YAP.

Keywords: Cc:$LuAlO_3$ (LuAP); Ce:$YAlO_3$ (YAP); Scintillators; Thermoluminescence; Cerium; Lutetium; Gamma radiation

1. Introduction

Lempicki et al. [1] expressed the efficiency of scintillator response, η, as the product of three partial efficiencies:

$$\eta = \beta S Q, \tag{1.1}$$

where β is the conversion efficiency (ratio of actually produced electron–hole pairs to maximum possible), S is the transfer efficiency and Q is the quantum efficiency of luminescence. More recently, Bartram and Lempicki [2] have demonstrated that efficient conversion ($\beta \cong 1$) is expected for wide-band-gap insulators. They have also shown that this prediction implies low transfer efficiency, $S < 1$, for most insulators. There are many processes in a solid which can diminish the efficiency of scintillator response by competing with prompt energy transfer to activators. One such process is explored in the present investigation of two closely related materials with contrasting efficiencies.

The desirable qualities of a scintillator material are high density, short decay time, and high light yield. Lempicki et al. [3] have compared the light outputs of two very similar scintillator materials of contemporary technological interest, Ce:$LuAlO_3$ (LuAP) and Cc:$YAlO_3$ (YAP). Both materials suffer from parasitic absorption which is minimal in thin samples. Relevant properties of these two materials are listed in Table 1. In principle, the

* Corresponding author. Tel.: 860 423 0662; fax: 203 486 3346; e-mail: rbartram@neca.com.

PII S0022-2313(97)00125-7

Table 1
Properties of scintillator materials investigated

	Ce:$LuAlO_3$ (LuAP)	Ce:$YAlO_3$ (YAP)
Density (g/cm^3)	8.34 [3]	5.55 [3]
Decay time (ns)	18 [3]	24 [3]
Light output (photons/McV)	21 000 (260% of BGO) [3]	34 000 (420% of BGO) [3]
Electron–hole pairs/MeV	55 556 [2]	58 097 [2]
Efficiency η	38%	59%

newer material, LuAP, whose scintillation properties were first reported by Lempicki et al. [4], should be superior by virtue of its greater stopping power and shorter decay time. Unfortunately, these advantages are partially offset by the fact that the maximum light output of LuAP at its present stage of development is substantially less than that of YAP. The measured light output per MeV [3] and the predicted numbers of electron–hole pairs per MeV [2] for both LuAP and YAP are also listed in Table 1, together with their respective efficiencies of scintillator response, η, taken as the ratio of these two quantities. Since both materials are wide-band-gap insulators, and efficient d $\rightarrow$f emission of Ce^{3+} is involved in both cases with nearly identical spectra, the inefficiencies are attributed primarily to low transfer efficiency.

Thermoluminescence has proved to be a useful adjunct to radioluminescence in the study of scintillator materials [5]. Recent thermoluminescence measurements on LuAP by Wisniewski et al. [6] and Drozdowski et al. [7] provide direct evidence for electron trapping in lieu of prompt radioluminescence in this material. Measurements performed at the University of Delft on 0.75% Ce:$LuAlO_3$, subjected to ^{60}Co gamma-ray irradiation and subsequently heated at a rate of 6 K s^{-1}, reveal a prominent glow peak at 530 K (257°C), a much weaker glow peak at 380 K (107°C), and a third, much weaker still, at 640 K (367°C). (The precise temperatures of glow peaks are a function of the heating rate.) A three-dimensional plot of emission intensity as a function of wavelength and temperature confirms that the glow curves are dominated by Ce^{3+} emission with essentially the same spectrum as that of the scintillation. Analysis of thermoluminescence spectra and glow curves from measurements such as these facilitates identification of the recombination center, permits confirmation of first-order kinetics, and provides information concerning thermal trap depths (activation energies) and frequency factors [8]. The glow peaks at 380 and 530 K were found to correspond to traps of depth 0.7 and 1.6 eV, respectively [7].

The present experiment was initiated with the more limited objective of determining the branching ratio of electron–hole pairs which contribute either to thermoluminescence or to scintillation. (It should be noted that these two processes do not exhaust the possibilities; others include processes which ultimately culminate in non-radiative recombination. Afterglow associated with shallow traps is included as a component of scintillation both in the present experiment, and, to a large extent, in the measurement of light output [3].) We rely on the detailed thermoluminescence measurements on LuAP described above, not only for the positions of the glow peaks, but also for the assurance that the thermoluminescence and scintillation spectra are identical, thus permitting direct comparison of integrated glow curves with scintillation light output, rather than absolute measurement of each. We have also extended the experiment to YAP, arguing from analogy, although detailed thermoluminescence experiments had not been performed previously on that material.

The experiment was motivated by the following fundamental questions, which arose naturally during the course of development of LuAP: Does electron trapping provide significant competition to scintillation in LuAP? Is it less effective in YAP? To what extent does the difference in electron trapping, if any, explain the difference in light output of these two materials? To what extent does electron trapping explain their departures from ideal efficiency?

Experimental methods are described in Section 2, and experimental results are presented in Section 3, and analyzed in Section 4. Conclusions derived from these results are presented in Section 5.

2. Experimental methods

The comparison of thermoluminescence and scintillation light outputs was facilitated by employing a common apparatus and detection scheme for both measurements. In addition, the following established properties of LuAP were exploited: identical Ce^{3+} emission spectra for both processes, and known glow-peak temperatures. YAP was assumed to have similar emission spectra, but the glow peaks were not known a priori. A schematic diagram of the experimental setup is presented in Fig. 1.

An electron Van de Graaff accelerator, operated at 1.0 MV and 1.0 μA, was employed as the primary radiation source. The electron beam was stopped by a 9 cm × 18 cm × 0.17 cm copper target, which served as nearly a point source for gamma rays. Although the Van de Graaff accelerator is much less stable than a radioactive source, that disadvantage is more than offset by convenient access to the sample chamber, which permitted both scintillation and thermoluminescence measurements to be performed in situ without moving the sample or changing the optics. It was thus feasible to make comparative rather than absolute measurements of integrated light output. An additional advantage of the accelerator is the flexibility to permit independent adjustments of gamma ray energy and intensity.

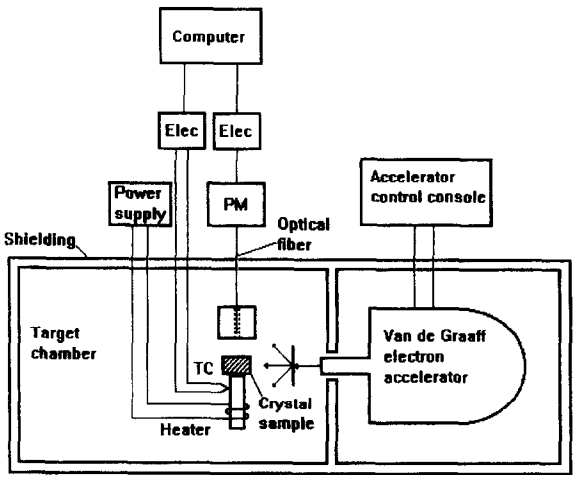

Fig. 1. Schematic diagram of experimental setup.

The single-crystal sample rested on the upper horizontal surface of a copper pedestal, in the form of a vertically aligned hollow right circular cylinder with a silver-brazed end cap, 0.75 cm in diameter and 5 cm long, partially enclosed by a 10 Ω power resister which served as a heating element. The nearest face of the sample was 2.5 cm from the copper target. A variac-controlled power supply with fixed setting provided a non-linear temperature ramp. Sample temperature was monitored by means of a copper-constantan thermocouple, hard soldered near the top of the pedestal. A compensator was employed in lieu of a cold junction.

Detection of luminescence was accomplished by a light guide in the form of a single-strand, clad and jacketed polymethyl methacrolate fiber, 30 ft long, with 2.0 mm i.d. and 3.0 mm o.d. The light guide was oriented at right angles to the direction of the electron beam, and the end surface facing the sample was embedded in a lead brick and recessed 3 mm. The remainder of the fiber was enclosed in lead-wrapped copper tubing within the target chamber, and was passed through the accelerator shielding to a Hamamatsu R928 photomultiplier tube outside. The transmission of the fiber in the wavelength range of the cerium emission was not measured, since absolute intensities were not required, but it proved to be much more than adequate for the purpose.

Both photomultiplier and thermocouple outputs were passed through Keithley 610C electrometers to a 486 personal computer. Data were acquired at 4 s intervals by means of Vernier's MPLI software and recorded on diskettes for subsequent processing.

The Van de Graaff accelerator was operated with manual regulation for periods ranging from 30 s to 16 min. The heat source was turned on immediately following each period of irradiation and turned off as soon as the sample temperature reached 290°C. Irradiation was resumed for the next run after the sample had cooled to approximately 34°C.

The Ce:$LuAlO_3$ sample was cut from a single-crystal boule, grown by Litton Airtron by the Czochralski method, to the dimensions 10 mm × 3 mm × 2 mm. The concentration of Ce^{3+} in the

starting materials was 0.75%, but the concentration in the crystal was only 15% of that, ~0.11% (600 ppmw). The Ce:$YAlO_3$ sample, grown by Union Carbide by the Czochralski method, was cut in the form of a right triangle with sides 10 mm × 11 mm × 17 mm and thickness 5.5 mm. Its measured concentration of Ce^{3+} is 0.5%. Both samples were pristine at the beginning of the experiment, with no history of prior irradiation or annealing. Samples were kept in the dark during irradiation and subsequent heating. It was also established that any given cycle of radiation and heating could be repeated with nearly identical results.

3. Experimental results

The ratio of scintillation signal to gamma-ray shot noise was approximately 40:1 for both samples, but the signal-to-noise ratio associated with thermoluminescence was orders of magnitude higher. In any event, gamma-ray shot noise and fluctuations associated with instability of the Van de Graaff accelerator were of no consequence to the experiment, since light outputs during scintillation and during each glow curve were integrated numerically. For presentation purposes only, light-output data during scintillation were triply smoothed to eliminate gamma-ray shot noise, but the fluctuations remain. Glow-curve and thermocouple-emf data were not smoothed. Thermocouple emfs were converted to Celsius temperatures by a standard formula [9].

Light output and temperature are plotted as functions of time for the following selected cases: a 4 min irradiation of LuAP in Fig. 2, a 16 min irradiation of LuAP in Fig. 3, and a 16 min irradiation of YAP in Fig. 4. The integrated scintillation light output is plotted as a function of irradiation time for LuAP in Fig. 5 and YAP in Fig. 6, and is seen to be reasonably linear in each case, in spite of accelerator instability.

The most prominent glow peak in Fig. 3 occurs at 235°C, with a much smaller peak at 90°C and a very weak shoulder with a broad maximum at 294°C, the highest temperature reached in the heating cycle. These temperatures are somewhat lower than those reported in Ref. [6] because of the lower

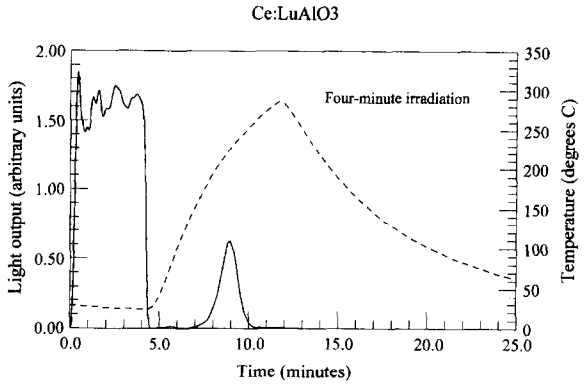

Fig. 2. Light output (continuous curve) and sample temperature (dashed curve) as functions of time for a 4 min irradiation of Ce:$LuAlO_3$.

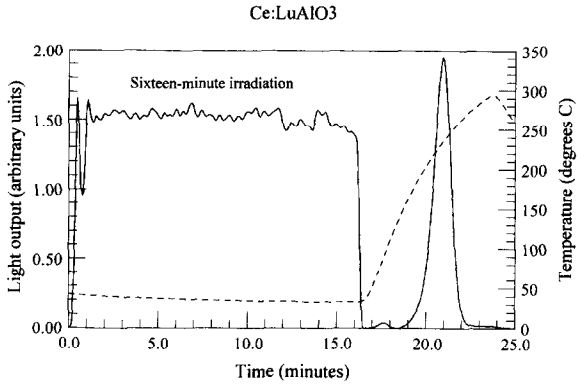

Fig. 3. Light output (continuous curve) and sample temperature (dashed curve) as functions of time for a 16 min irradiation of Ce:$LuAlO_3$.

heating rate employed in the present experiment, less than 1 K s^{-1}. The electron traps corresponding to the first two peaks are thoroughly emptied during each heating cycle, but that condition may not be fully satisfied for the shoulder. The contribution of this shoulder was combined with that of the prominent glow peak in calculating integrated light output.

The glow peaks in YAP, shown in Fig. 4, are much less prominent than those in LuAP and occur at different temperatures. Two nearly equal glow peaks are observed at 141°C and 206°C; to the best

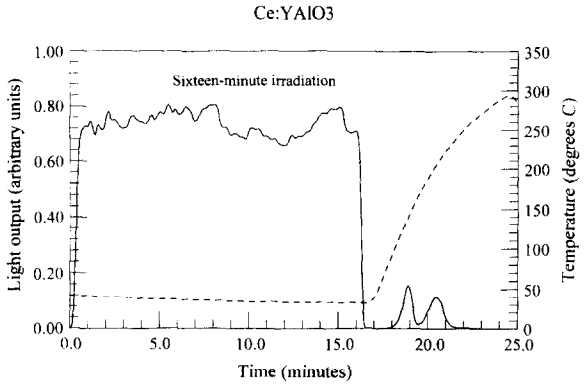

Fig. 4. Light output (continuous curve) and sample temperature (dashed curve) as functions of time for a 16 min irradiation of $Ce:YAlO_3$.

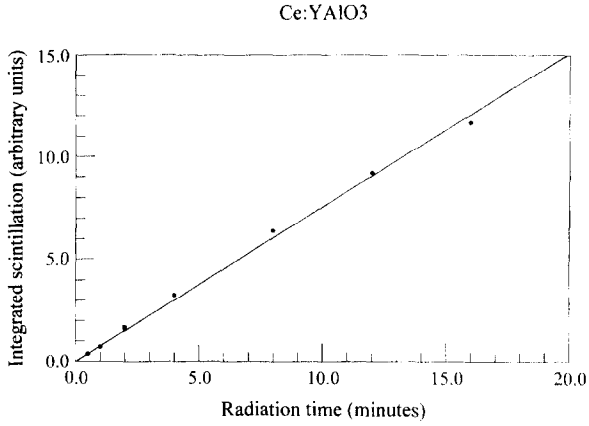

Fig. 6. Integrated scintillation light output as a function of radiation time for $Ce:YAlO_3$.

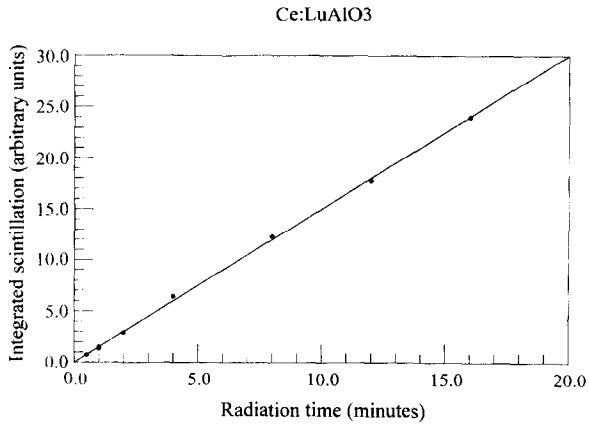

Fig. 5. Integrated scintillation light output as a function of radiation time for $Ce:LuAlO_3$.

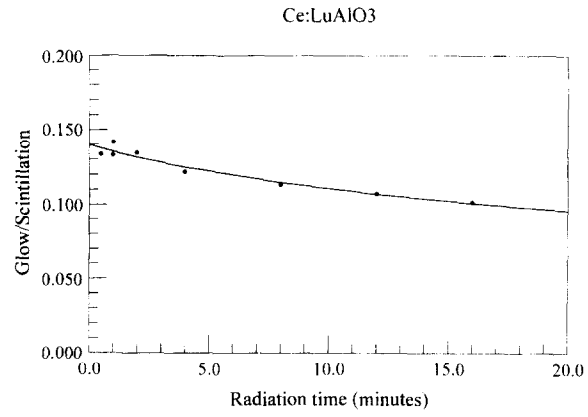

Fig. 7. Ratio of integrated light output under glow curves to integrated scintillation light output as a function of radiation time for $Ce:LuAlO_3$. The continuous curve is a plot of Eq. (7) with parameters adjusted for a least-squares fit to the data.

of our knowledge, these glow peaks have not been reported previously. We cannot discount the possibility of additional glow peaks in YAP above 300°C.

It is evident from comparison of Figs. 2 and 3 that the glow peaks in LuAP increase in height in approximate proportion to the duration of irradiation; thus the relevant electron traps are far from saturated. To address this point more precisely, the ratio of integrated light output under both glow curves to the integrated scintillation light output (G/S) is plotted as a function of radiation time for LuAP in Fig. 7 and for YAP in Fig. 8. This ratio declines gradually and non-linearly with radiation time, and its initial value is very much larger for LuAP (0.14) than for YAP (0.02). The ratio of integrated light output under the low-temperature glow curve to that under the high-temperature glow curve, 0.013 for LuAP and 0.88 for YAP, is essentially independent of radiation time for both materials.

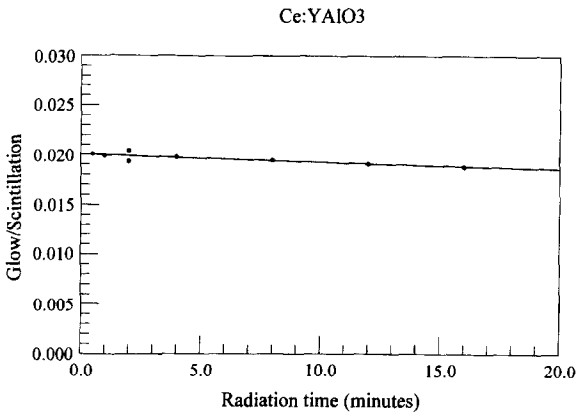

Fig. 8. Ratio of integrated light output under glow curves to integrated scintillation light output as a function of radiation time for Ce:$YAlO_3$. The continuous curve is a plot of Eq. (7) with parameters adjusted for a least-squares fit to the data.

4. Analysis

Direct comparison of integrated thermoluminescence and scintillation light outputs reveals that the initial value of their ratio, G/S, is much larger in LuAP, 0.14, than in YAP, 0.02. In the absence of electron trapping, the efficiency of scintillator response, η, would increase from 38% to 43% in LuAP and from 59% to 60% in YAP. Additional processes culminating in non-radiative recombination may account for the residual discrepancy between ideal and actual efficiency of luminescence.

Although it is not clear at what stage in the process non-radiative recombination occurs, it does not appear to be associated with thermal quenching of luminescence, since the emission lifetimes are temperature invariant. Accordingly, it is attributed to trapping of holes at distinct non-radiative recombination centers. The dependence of G/S on radiation time in Figs. 7 and 8 can be explained by a simple model in which the electron trapping process is described by the following five rate equations, adapted from Ref. [10]:

$$\frac{dn_c}{dt} = f - n_c n_R A_{rR} - n_c n_{NR} A_{rNR} - n_c(N - n) A, \quad (1a)$$

$$\frac{dn}{dt} = n_c(N - n) A, \quad (1b)$$

$$\frac{dn_v}{dt} = f - n_v(N_R - n_R) A_{hR} - n_v(N_{NR} - n_{NR}) A_{hNR}, \quad (1c)$$

$$\frac{dn_R}{dt} = n_v(N_R - n_R) A_{hR} - n_c n_R A_{rR}, \quad (1d)$$

$$\frac{dn_{NR}}{dt} = n_v(N_{NR} - n_{NR}) A_{hNR} - n_c n_{NR} A_{rNR}, \quad (1e)$$

where f is the rate of production per unit volume of electron–hole pairs, n_c is the concentration of electrons in the conduction band, n_v is the concentration of holes in the valence band, n_R is the concentration of holes trapped on radiative recombination centers, n_{NR} is the concentration of holes trapped on non-radiative recombination centers, n is the concentration of trapped electrons, and N, N_R and N_{NR} are, respectively, the concentrations of electron traps, radiative recombination centers and non-radiative recombination centers. The coefficient A determines the rate of trapping of conduction electrons, A_{hR} determines the rate of trapping of valence-band holes at radiative recombination centers, A_{hNR} determines the rate of trapping of valence-band holes at non-radiative recombination centers, A_{rR} determines the rate of radiative recombination of conduction electrons with trapped holes, and A_{rNR} determines the rate of non-radiative recombination of conduction electrons with trapped holes. A subsidiary condition is

$$\frac{dn_c}{dt} + \frac{dn}{dt} = \frac{dn_v}{dt} + \frac{dn_R}{dt} + \frac{dn_{NR}}{dt}. \quad (1f)$$

Since these rate equations obviously contain too many adjustable parameters, it is necessary to introduce arbitrary simplifying assumptions. We first assume that the coefficients which determine the hole trapping and recombination rates are the same for both radiative and non-radiative recombination centers, $A_{hR} = A_{hNR} \equiv A_h$ and $A_{rR} = A_{rNR} = A_r$, and we define $N_h \equiv N_R + N_{NR}$ and $n_h \equiv n_R + n_{NR}$ to be the total concentration of hole traps and the total concentration of trapped holes, respectively. With these assumptions, Eqs. (1) are reduced to

$$\frac{dn_c}{dt} = f - n_c n_h A_r - n_c(N - n) A, \quad (2a)$$

$$\frac{dn}{dt} = n_c(N-n)A, \tag{2b}$$

$$\frac{dn_v}{dt} = f - n_v(N_h - n_h)A_h, \tag{2c}$$

$$\frac{dn_h}{dt} = n_v(N_h - n_h)A_h - n_c n_h A_r, \tag{2d}$$

$$\frac{dn_c}{dt} + \frac{dn}{dt} = \frac{dn_v}{dt} + \frac{dn_h}{dt}. \tag{2e}$$

Eqs. (2) can be simplified further by assuming that trapping of valence-band holes occurs on a much shorter time scale than all other processes ($A_h \to \infty$, $n_v \to 0$). We also found it necessary to assume an initial concentration of trapped holes, n_{h0}, presumably charge compensated by cation vacancies or impurities; otherwise, electron trapping would be completed in a very short time and G/S would exhibit nearly parabolic time dependence. With the additional assumption that these initial trapped holes are distributed between radiative and non-radiative recombination centers in proportion to their concentrations, the parameters associated with non-radiative recombination are reduced to the single available datum, the overall efficiency of luminescence, ε, the same for both scintillation and thermoluminescence, given by

$$\varepsilon = \frac{N_R}{N_R + N_{NR}}. \tag{3}$$

The parameters in Eqs. (2) are constrained by the known rapidity of scintillator response. In particular, transients associated with the recombination term $-n_c n_h A_r$ in Eq. (2a) must die out in tens of nanoseconds. Eq. (2a) then has the approximate quasi-equilibrium solution

$$n_c \cong \frac{f}{(n_{h0}+n)A_r + (N-n)A}, \tag{4}$$

and Eq. (2b) can be approximated by

$$\frac{dn}{dt} \cong \left(\frac{f}{(n_{h0}+n)A_r + (N-n)A}\right)(N-n)A. \tag{5}$$

The scintillation light output was found to be independent of radiation time to a good approximation; consequently, the integrated scintillation light output, S, is given by

$$S \cong \varepsilon\left(\frac{n_{h0}A_r}{n_{h0}A_r + NA}\right)ft(\text{photons}), \tag{6a}$$

and the integrated glow curve is given by

$$G = \varepsilon n(\text{photons}). \tag{6b}$$

Eq. (5) was solved by numerical integration for various values of the ratio N/n_{h0}, with the parameters $\alpha = NA/n_{h0}A_r$ and $\beta = fA/(n_{h0}A_r + NA)$ adjusted for a least-squares fit of $G/S = (\alpha/\beta)(n/Nt)$ to the corresponding data for LuAP. Although a plausible fit is obtained in each case, the best fit, and certainly the most convincing qualitative representation of apparent trends in the LuAP data, are obtained in the limit $N \gg n_{h0}$. In this limit, Eq. (5) has the following closed-form solution:

$$G/S = \frac{(1+\alpha)}{\delta t}\left[-(1+\alpha) + \sqrt{(1+\alpha)^2 + 2\alpha\delta t}\right], \tag{7}$$

where $\delta = f/n_{h0}$. The continuous curves in Figs. 7 and 8 are plots of Eq. (7) with the parameters adjusted for a least-squares fit to the data. Optimum parameter values are $\alpha = 0.1397$ and $\delta = 0.622\,\text{min}^{-1}$ for LuAP and $\alpha = 0.02002$ and $\delta = 0.434\,\text{min}^{-1}$ for YAP. The gradual decline of G/S with radiation time is due to an increase in the concentration of trapped holes, n_h, and a corresponding decrease in the concentration of conduction electrons, n_c, to compensate for the increasing concentration of trapped electrons, n, while maintaining a constant rate of recombination, rather than to saturation of electron traps.

The fitted parameters provide a value of the ratio f/n_{h0}. In order to facilitate absolute determination of n_{h0}, we proceed to estimate f, the rate of production of electron–hole pairs per unit volume, for LuAP. For a relativistic electron and negligible screening of target nuclei, the ratio of differential energy loss to radiation and collisions is [11]

$$\frac{dE_{rad}}{dE_{coll}} = \left(\frac{4Z\ln(2\gamma)}{3\pi(137)\ln(\gamma^2 mc^2/\hbar\omega)}\right)\gamma, \tag{8a}$$

$$\gamma \equiv E/mc^2, \tag{8b}$$

where Z is the atomic number of the target atom (29 for copper) and $\hbar\omega$ is a characteristic energy of its valence electrons, which we assume to be ~ 10 eV. Neglecting the γ dependence of the logarithms, which are slowly varying, one obtains

$$E_{\mathrm{rad}} \cong (mc^2)\left(\frac{4Z\ln(2\gamma_0)}{3\pi(137)\ln(\gamma_0^2 mc^2/\hbar\omega)}\right)\frac{\gamma_0^2}{2} \cong 0.01 \text{ MeV}, \tag{9}$$

where $\gamma_0 \cong 2$ is the initial value of γ.

It follows from Eq. (9) that, of the 1 W power of the incident electron beam, only 10 mW is converted to gamma radiation. This radiation is confined to a cone of half-angle γ_0^{-1}, impinging on an area $\pi d^2/\gamma_0^2$ at a distance d from the target. Accordingly, 2.0 mW cm^{-2} is incident on a sample 2.5 cm from the target.

The sample penetration depends on photon energy, which is distributed non-uniformly below 1 MeV. The maximum energy is just below the threshold for electron–positron pair production, and Compton scattering is the dominant interaction mechanism over most of the energy range [12]. The Thomson cross section σ_T, given by [13]

$$\sigma_T = \frac{8\pi}{3}\left(\frac{e^2}{mc^2}\right)^2 = 6.65\times 10^{-25}\ \mathrm{cm}^2, \tag{10}$$

is an upper bound on the Compton cross section at all energies. Since the electron concentration in LuAP is $N_e = 2.17\times 10^{24}$ cm^{-3}, the penetration depth L satisfies the inequality $L > (N_e\sigma_T)^{-1} = 0.69$ cm. This result is corroborated by an independent determination, made with a computer program and data base developed at NIST [14], which yields an absorption coefficient of 1.0 cm^{-1} for 0.5 MeV gamma rays. Accordingly, the penetration depth is approximately $L = 1.0$ cm and the rate of energy deposition is approximately 2.0 mW/cm^3. This result can be combined with the theoretical prediction of 55 556 electron–hole pairs per MeV in LuAP [2] to yield $f \cong 5\times 10^{16}$ cm^{-3} min^{-1}. For comparison, the concentration of lutetium sites is 2.0×10^{22} cm^{-3} and the cerium concentration is 2.3×10^{19} cm^{-3}.

From the fitted parameters and the estimate of f, we infer the value $n_{h0} \cong 1.2\times 10^{17}$ cm^{-3}, a result which implies that the pre-existing concentration of trapped holes is approximately 3 ppmw, comparable with known impurity concentrations in LuAP. [The most abundant impurities are Y (30 ppmw), Yb (8 ppmw), Gd (7 ppmw), and Si (3 ppmw).] Since approximately 10% of the electrons produced are trapped following a 16 min irradiation, the number of trapped electrons in that case is $n \cong 8\times 10^{16}$ cm^{-3}. The initial rate of electron trapping is

$$\left(\frac{dn}{dt}\right)_{t=0} = n_{c0}NA = \left(\frac{\alpha}{1+\alpha}\right)f \cong 6\times 10^{15}\ \mathrm{cm}^{-3}\,\mathrm{min}^{-1}. \tag{11}$$

Additional empirical information permits further progress; the fact that the 18 ns scintillation response time of LuAP is dominated by the radiative lifetime of Ce^{3+} imposes a lower bound on the recombination rate $n_{h0}A_r$. Estimates based on the measured rise time, 0.8 ns [15], are $n_{h0}A_r = 7.5\times 10^{10}$ min^{-1} and $NA = \alpha n_{h0}A_r = 10^{10}$ min^{-1}. Consequently, it follows from Eq. (11) that the initial concentration of conduction electrons is $n_{c0} = 6\times 10^5$ cm^{-3}.

The preceding considerations fail to provide values of N and A independently, apart from the requirement $N \gg 1.2\times 10^{17}$ cm^{-3}. Among the possible candidates for electron traps, it is important to distinguish between one of the more abundant impurities, such as Y^{3+}, and the Ce^{3+} dopant, which may also be stable in its 2+ charge state [16], in order to assess the feasibility of eliminating unwanted electron trapping. Unfortunately, that information is not provided by the present experiment.

Since the thermoluminescence of YAP has not been reported previously, it is of interest to analyze the data obtained in the present experiment. Thermoluminescence measurements on LuAP [7, 8] had been performed with a linear temperature ramp to facilitate analysis in terms of a closed-form expression for the glow curve. However, there is no inherent difficulty in analyzing glow curves obtained with a non-linear temperature ramp, such as those in the present experiment, provided that the temperature, $T(t)$, is known as a function of time. The two overlapping glow curves in Fig. 4 were simulated by numerical integration, with a 4 s

time interval, of the rate equations

$$\frac{d(n_i/n_0)}{dt} = -(n_i/n_0)s_i \exp(-E_i/kT), \tag{12a}$$

$$n = n_1 + n_2, \tag{12b}$$

subject to the initial conditions

$$n_{10}/n_0 = \frac{G_1/G_2}{1 + G_1/G_2}, \tag{13a}$$

$$n_{20}/n_0 = \frac{1}{1 + G_1/G_2}, \tag{13b}$$

where $G_1/G_2 = 0.859$ is the ratio of integrated light outputs for the two glow curves. These equations assume first-order kinetics; i.e., the process is controlled solely by the release of electrons from two traps with concentrations n_1 and n_2, because an excess of recombination centers (trapped holes) is available. Initial values are denoted by the subscript 0. The theoretical normalized light output, $-d(n/n_0)/dt$, was then compared with the normalized double glow curve, and the parameters $\ln s_1$, E_1, $\ln s_2$, E_2 were adjusted for a least-squares fit, as shown in Fig. 9. The quality of the fit supports the assumption of first-order kinetics. The optimum values of the parameters are listed in Table 2. It was unnecessary to correct the glow curves for thermal quenching, since the glow peaks occur well below the quenching temperature, 590 K [17].

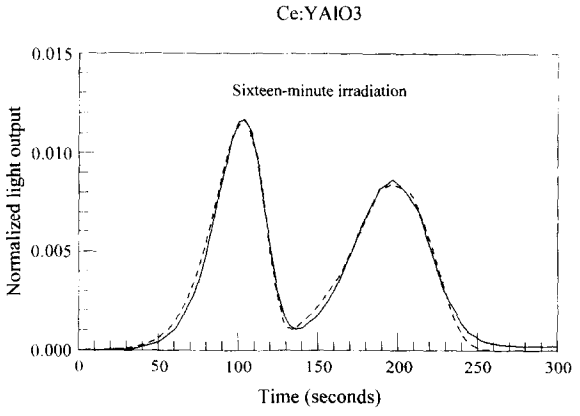

Fig. 9. Comparison of simulated (dashed line) and experimental (solid line) glow curves in Ce:$YAlO_3$ following a 16 min irradiation. The simulation is accomplished by numerical integration of Eqs. (12). Optimized parameters for the simulated glow curves, adjusted for a least-squares fit to the data, are listed in Table 2.

Table 2
Optimized thermoluminescence parameters for Ce:$YAlO_3$ (YAP), derived from least-squares fit to glow curves following 16 min irradiation (Fig. 9)

Parameter	First glow curve	Second glow curve
Glow-peak temp. (°C)	141	206
$\ln s$	26.58	27.35
E (eV)	1.05	1.27

5. Summary and conclusions

Direct comparison of integrated thermoluminescence and scintillation light outputs reveals that their ratio, G/S, is much larger in LuAP, 0.14, than in YAP, 0.02. In the absence of electron trapping, the efficiency of scintillator response, η, would increase from 38% to 43% in LuAP and from 59% to 60% in YAP. Thus the results of the present experiment establish that electron trapping provides significant competition to radioluminescence in these two scintillator materials, but it accounts only partially for their performance differential and their departures from ideal efficiency. Additional processes culminating in non-radiative recombination may also depress transfer efficiency. It is known from previous work that the dominant trap in LuAP has a depth of 1.6 eV [7]. Analysis of glow curves in YAP reveals two traps with comparable concentrations of trapped electrons and with depths of 1.05 and 1.27 eV.

The comparative measurements performed here on LuAP provide evidence for pre-existing trapped holes (Ce^{4+} for radiative recombination and an unknown center for non-radiative recombination). Although they do not conclusively determine the ratio of the initial concentration of trapped holes, n_{h0}, to the concentration of potential electron traps, N, the preferred fit suggests that n_{h0} is comparable with known impurity concentrations and that N is

much larger than n_{h0}, possibly implicating either Y^{3+} or Ce^{3+} as the electron trap. Interpretation of these measurements also suggests that suppression of electron trapping may be accomplished by deliberately increasing the initial concentration of trapped holes, n_{h0}, in order to diminish the concentration of conduction electrons, n_c. That would have the effect of reducing the parameter α, and consequently reducing G/S.

The experiment reported here was performed on a single sample of each material. Since the properties of these scintillator materials are known to be strongly sample dependent, it would be useful to repeat the experiment on a variety of samples, especially some of differing cerium concentration, higher purity and intentional doping, in order to confirm and extend the present conclusions. Additional measurements are anticipated as part of a continuing program of materials development.

Acknowledgements

This research was supported by the National Institutes of Health under Grant #1R43CA71228-01.

References

[1] A. Lempicki, A.J. Wojtowicz, E. Berman, Nucl. Instr. and Meth. A 333 (1993) 304.
[2] R.H. Bartram, A. Lempicki, J. Lumin. 68 (1996) 225.
[3] A. Lempicki, C. Brecher, D. Wisniewski, E. Zych, in: P. Dorenbos, C.W.E. van Eijk (Eds.), Proc. Int. Conf. on Inorganic Scintillators and their Applications, SCINT95, Delft 1995, Delft University Press, Delft (Netherlands), 1996, p. 340.
[4] A. Lempicki, M.H. Randles, D. Wisniewski, M. Balcerzyk, C. Brecher, A.J. Wojtowicz, IEEE Nucl. Sci. 42 (1995) 280.
[5] P. Dorenbos, C.W.E. van Eijk, A.J.J. Bos, C.L. Melcher, J. Lumin. 60, 61 (1994) 979.
[6] D. Wisniewski, W. Drozdowski, A.J. Wojtowicz, A. Lempicki, P. Dorenbos, J.T.M. de Haas, C.W.E. van Eijk, A.J.J. Bos, Acta Phys. Pol. A 90 (1996) 377.
[7] W. Drozdowski, D. Wisniewski, A.J. Wojtowicz, A. Lempicki, P. Dorenbos, J.T.M. de Haas, C.W.E. van Eijk, A.J.J. Bos, Proc. Int. Conf. on Luminescence, Prague, 1996; J. Lumin., in press.
[8] S.W.S. McKeever, Thermoluminescence of Solids, Cambridge University Press, Cambridge, 1985.
[9] David R. Lide, (Ed.), CRC Handbook of Chemistry and Physics, 74th ed., 1993–94, p. 15-13.
[10] S.W.S. McKeever, op. cit., p. 45.
[11] J.D. Jackson, Classical Electrodynamics, Wiley, New York, 1962, p. 519.
[12] G. Blasse, B.C. Grabmaier, Luminescent Materials, Springer Berlin, Heidelberg, 1994, p. 171.
[13] J.D. Jackson, op. cit., p. 489.
[14] M.J. Berger, J.H. Hubbell, Center for Radiation Research, NIST, private communication.
[15] S.E. Derenzo, W.W. Moses, M.J. Weber, A.C. West, C. Dujarddin, Conference Record, IEEE Nucl. Sci. Symp. and Medical Imag. Conf., San Francisco, October 1995.
[16] R.C. Alig, Z.J. Kiss, J.P. Brown, D.S. McClure, Phys. Rev. 186 (1969) 276.
[17] Li-Ji Lyu, D.S. Hamilton, J. Lumin. 48, 49 (1991) 251.